

Supporting Information for

**A large  $\pi$ -conjugated ligand in metal-organic framework as opticalswitch to regulate the electron transfer pathway for highly selective reduction of CO<sub>2</sub> to CH<sub>4</sub>**

Yuan-Yuan Liu, Hao-Lin Zhu, Ning-Yu Huang, Pei-Qin Liao,\* Xiao-Ming Chen

*MOE Key Laboratory of Bioinorganic and Synthetic Chemistry, School of Chemistry, Sun Yat-Sen University, Guangzhou 510275, China*

\*E-mail: liaopq3@mail.sysu.edu.cn

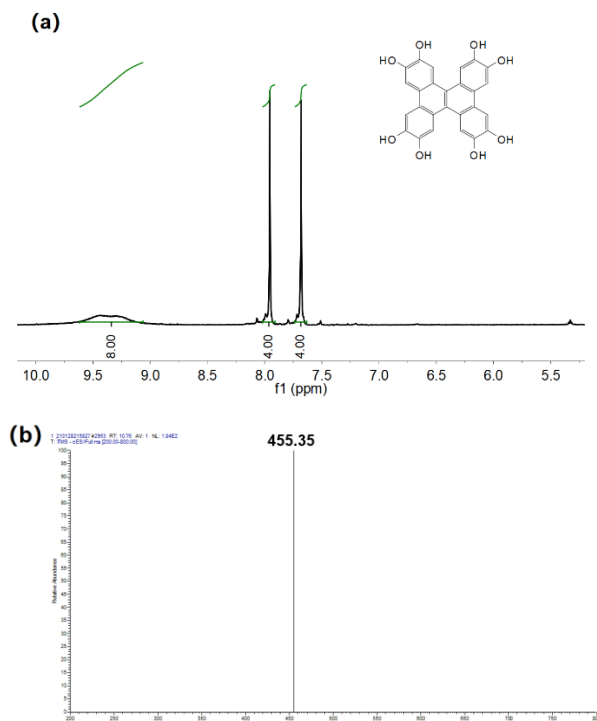


**Figure S1.** (a-b)  $^1\text{H}$  nuclear magnetic resonance ( $^1\text{H}$  NMR) spectrum and mass spectrum of H<sub>8</sub>dbc.  $^1\text{H}$  NMR (400 MHz, DMSO)  $\delta$  (ppm): 7.68(s, 4H), 7.95 (s, 4H) and 9.37 (s,8H). The successful synthesis of H8DBC were demonstrated by the  $^1\text{H}$  NMR spectrum and Mass spectrum.

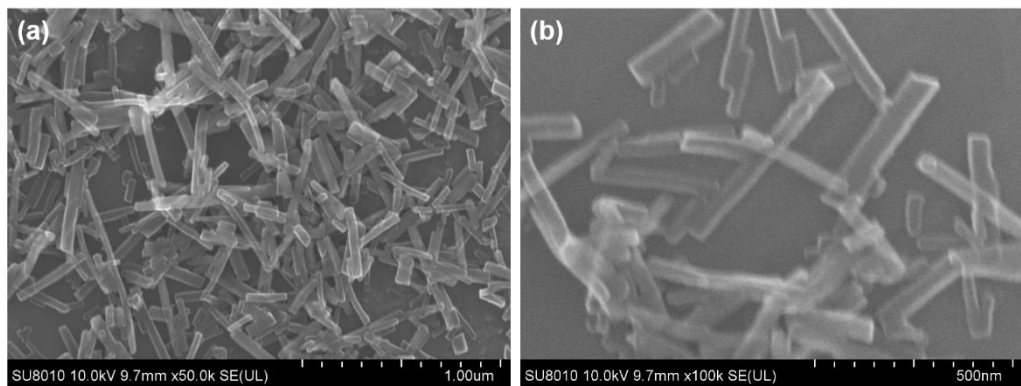


**Figure S2.** (a-b) SEM images of **Cu-DBC**.

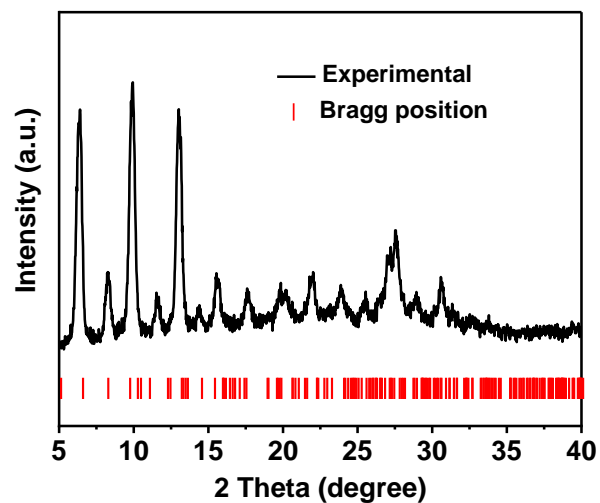


**Figure S3.** PXRD pattern of **Cu-DBC**.

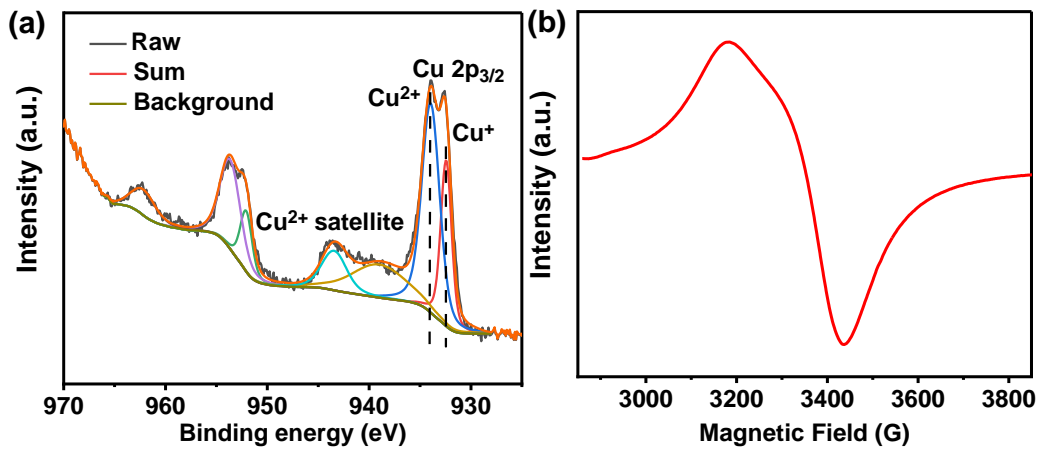


**Figure S4.** (a) Cu 2p XPS spectrum of Cu-DBC. (b) EPR spectrum of solid Cu-DBC.

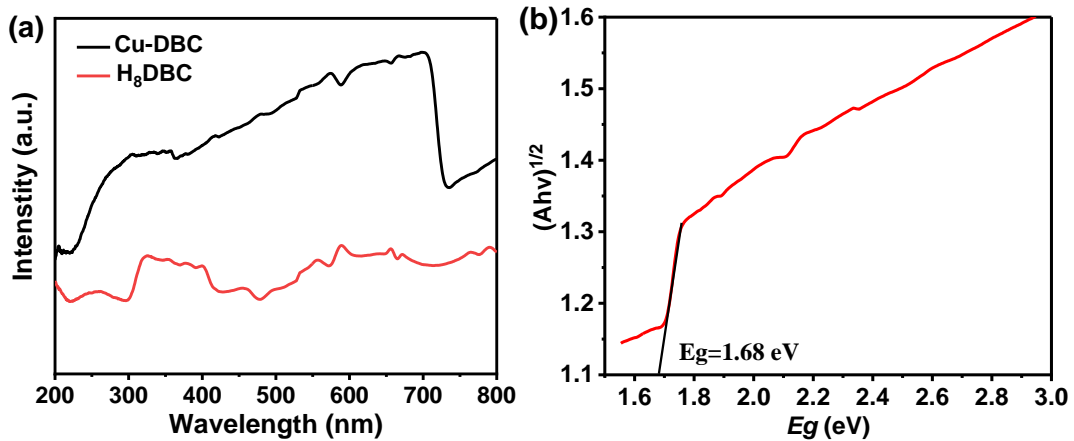


**Figure S5.** (a) UV-vis diffuse reflectance spectra of Cu-DBC and H<sub>8</sub>dbc. (b) The Tauc plot of Cu-DBC.

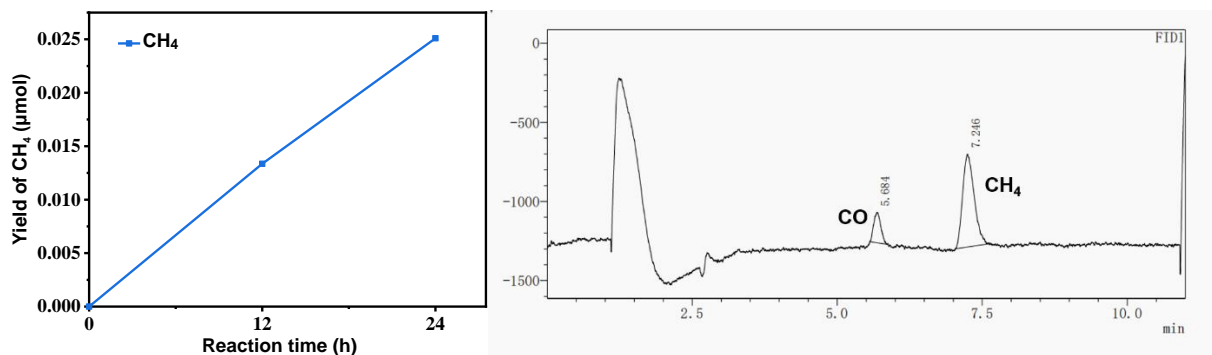


**Figure S6.** CH<sub>4</sub> production rate of photocatalytic CO<sub>2</sub> reduction by **Cu-DBC** (left) and GC spectrum of photocatalytic production (right) and  $n(\text{CH}_4) = 0.025 \text{ } \mu\text{mol}$ ,  $n(\text{CO}) = 3.08 \times 10^{-5} \text{ } \mu\text{mol}$ . Reaction condition: catalyst (1 mg), solvent (5 mL, CH<sub>3</sub>CN/H<sub>2</sub>O = 4:1), triethanolamine (TEOA, 0.1 mol), LED light ( $\lambda = 420 \text{ nm}$ ), 1.0 atm (pure CO<sub>2</sub>).

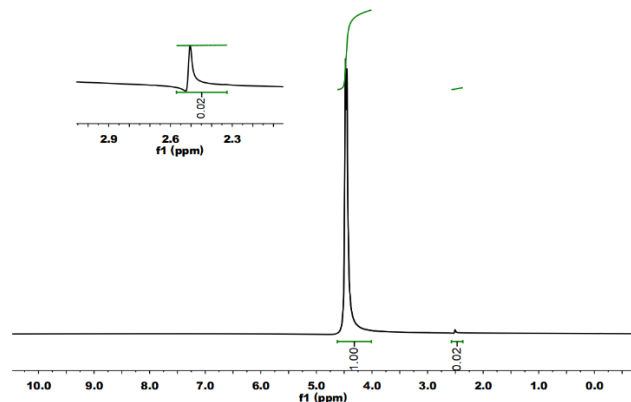


**Figure S7.** The <sup>1</sup>H nuclear magnetic resonance (<sup>1</sup>H NMR) spectrum of the liquid phase in electrocatalytic CO<sub>2</sub> reduction.

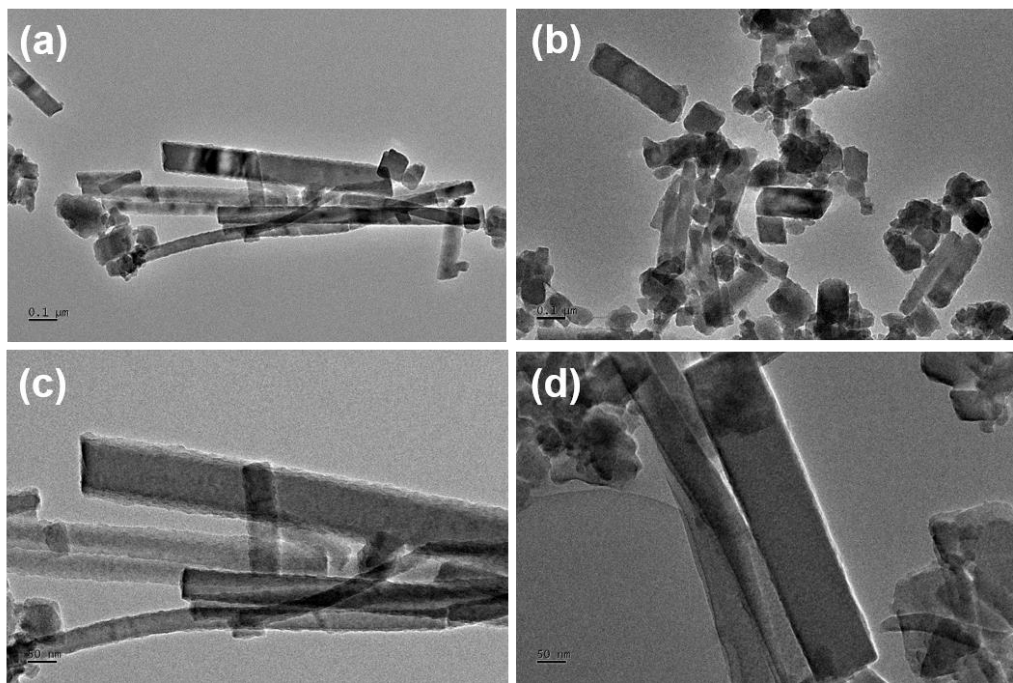


**Figure S8.** (a, c) TEM images of **Cu-DBC**. (b, d) TEM images of **Cu-DBC** after  $\text{CO}_2$  reduction at  $-1.4 \text{ V vs. RHE}$  for 2.5 h.

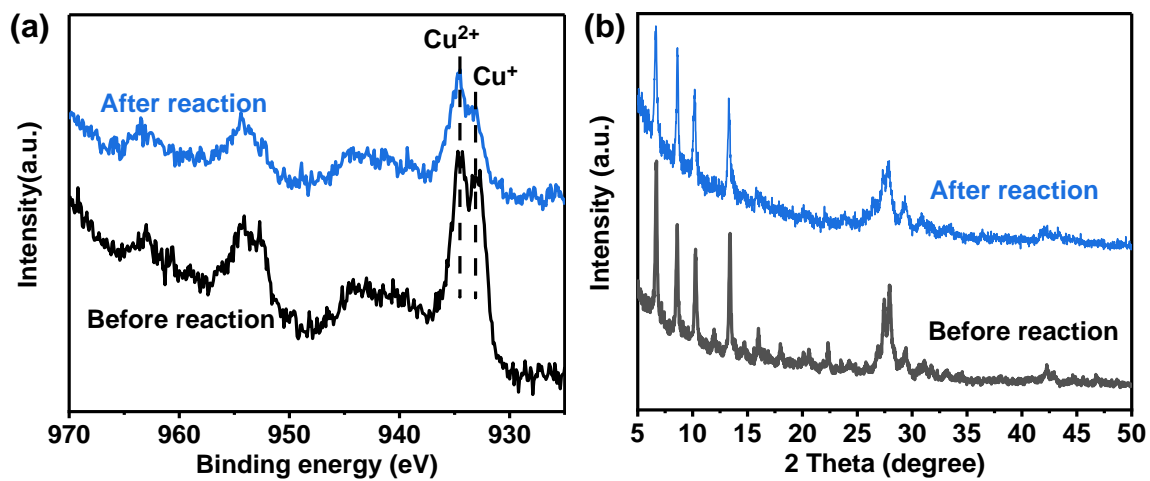


**Figure S9.** (a-b) Cu 2p XPS spectra and PXRD patterns of **Cu-DBC** before and after  $\text{CO}_2$  reduction at  $-1.4 \text{ V vs. RHE}$  for 2.5 h.

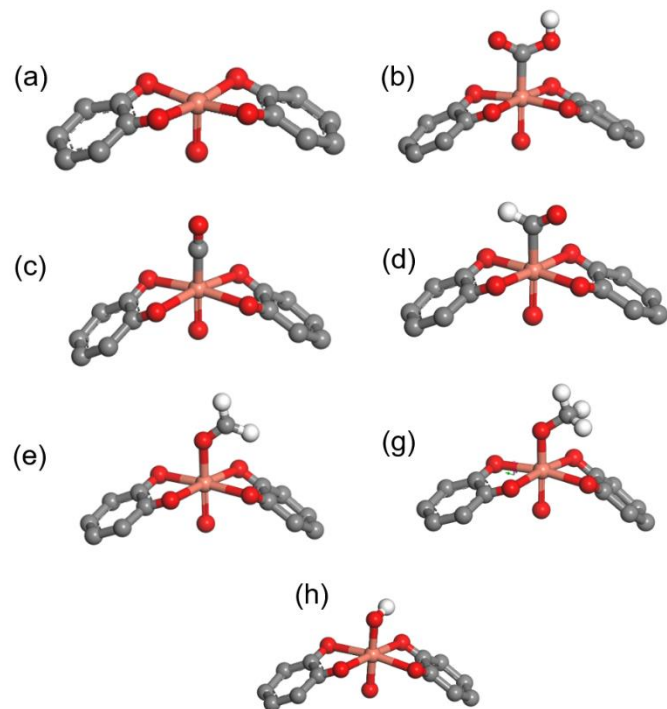


**Figure S10.** Illustration of intermediates in electrocatalytic CO<sub>2</sub>RR, which represent \* (a), \*COOH (b), \*CO (c), \*CHO (d), \* OCH<sub>2</sub> (e), \*OCH<sub>3</sub> (f), and \*OH (g) intermediates.

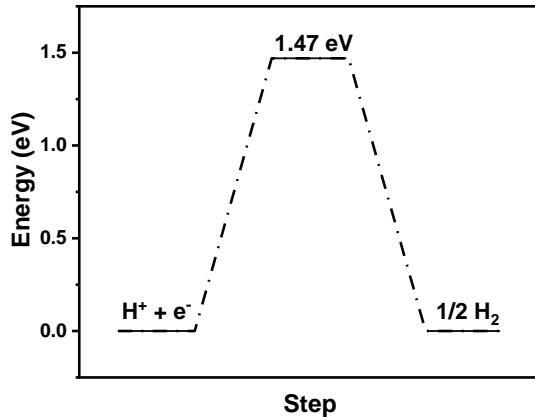


**Figure S11.** Illustration of the energy barrier of hydrogen evolution reaction of **Cu-DBC**.

**Table S1.** Summary of the reported systems of photo-coupled electrocatalytic and electrocatalytic CO<sub>2</sub> reduction.

Catalyst	Electrocatalyst	Electrolyte	Main product	Potential	FE	Reference
PECR catalyst	Cu-DBC	0.1 M KHCO <sub>3</sub>	CH <sub>4</sub>	-1.0 V	84.3%	This work
				-1.2 V	88.6%	
				-1.4 V	93.2%	
	Ag-supported dendritic Cu	0.1 M CsHCO <sub>3</sub>	Hydrocarbons	-1.0 V <i>vs</i> SCE	79 ± 6%	<sup>2</sup>
	Porphyrin-Au	0.1 M KHCO <sub>3</sub>	CO	-0.9 V	94%	<sup>3</sup>
	CoPc-Rs/Fe <sub>2</sub> O <sub>3</sub> NTs	0.1 M KHCO <sub>3</sub>	CH <sub>3</sub> OH	-1.3V	84%	<sup>4</sup>
	NiPc-TFPN COF	0.5 M KHCO <sub>3</sub>	CO	-0.9 V	99%	<sup>5</sup>
	GaN:Sn	0.1 M KHCO <sub>3</sub>	HCOOH	-0.53 V	76%	<sup>6</sup>
	FeS <sub>2</sub> /TiO <sub>2</sub> NTs	0.1 M KHCO <sub>3</sub>	CH <sub>3</sub> OH	-1.2 V.SCE	39.8%	<sup>7</sup>
	FN-CTF-400	0.1 M KHCO <sub>3</sub>	CH <sub>4</sub>	-0.7 ~ -0.9 V	99.3%	<sup>8</sup>
Electrocatalysts	Cu/MoS <sub>2</sub>	0.1 M NaHCO <sub>3</sub>	CO	-0.8 V	35.2%	<sup>9</sup>
	CuO <sub>x</sub> nanoparticle	0.1 M KHCO <sub>3</sub>	C <sub>2</sub> H <sub>4</sub>	-1.0 V	21%	<sup>10</sup>
	Cu <sub>2</sub> O@CuHHTP	0.1 M KCl/0.1 M KHCO <sub>3</sub>	CH <sub>4</sub>	-1.4 V	73%	<sup>11</sup>
	Cu phthalocyanine	0.5 M KHCO <sub>3</sub>	CH <sub>4</sub>	-1.06 V	66%	<sup>12</sup>
	Pd/Cu <sub>2</sub> O-Cu	0.5 M NaHCO <sub>3</sub>	CH <sub>4</sub>	-0.65 V	30%	<sup>13</sup>

Notes: The potentials mentioned in this table are based on the reversible hydrogen electrode (RHE) unless otherwise stated. All the reported electrocatalysts at the listed potentials exhibited maximum product selectivity.

## Experimental section

**Materials and general methods.** The ligand dibenzo-[g,p]chrysene-2,3,6,7,10,11,14,15-octaol was synthesized according to the literature<sup>1</sup> Other reagents were commercially available and without further purification. Powder X-ray diffraction (PXRD) patterns were collected on a Bruker D8 Advance diffractometer (Cu K $\alpha$ ). X-ray photoelectron spectroscopy (XPS) measurements were performed on an ESCALAB 250 spectrometer. A SU8010 scanning electron microscope was utilized to investigate the morphology of Cu-DBC. High resolution images of microcrystalline powder of Cu-DBC before and after CO<sub>2</sub> reduction reaction were obtained by a transmission electron microscope (TEM). <sup>1</sup>H Nuclear magnetic resonance (<sup>1</sup>H NMR) measurements were performed on a Bruker advance III. Attenuated total reflection infrared (ATR-FTIR) spectra were recorded on a Nicolet 6700 (Thermo Fisher) to study the reaction intermediates formed over Cu-DBC in the electrochemical measurements.

**Synthesis of Cu-DBC.** dibenzo-[g,p]chrysene-2,3,6,7,10,11,14,15-octaol (8.6 mg) and Cu(OAc)<sub>2</sub> (6 mg) were dissolved in 500  $\mu$ L DMF and 2 mL deionized water. After ultrasonic treatment for 30 minutes, the vessel was placed in an oven with the temperature of 85 °C for 72 hours. Then the MOF was separated from the reaction mixtures by washing with water and dried overnight in 60 °C to obtain the black product.

**Photochemical experiments:** Cu-DBC (1 mg) was dispersed in a mixed solution (5 ml, CH<sub>3</sub>CN/H<sub>2</sub>O = 4:1), with ultrasonication for 30 min. The suspension was added 0.1 mol triethanolamine (TEOA), and then purged by CO<sub>2</sub> gas at a pressure of 1 atm for 30 min. The reaction mixture was continuously stirred with a magneton and irradiated under a LED light with a wavelength of 420 nm. The reaction gaseous products were analyzed by a gas chromatography (Agilent 7890B).

**Electrocatalytic CO<sub>2</sub> reduction.** All the electrochemical measurements were conducted with a CHI660E chemical workstation and the H-type cell was used as the electrolyzer for electrocatalytic CO<sub>2</sub> reduction. The preparation methods of working electrode is as follows: Cu-DBC (5 mg) was dispersed in 500  $\mu$ L isopropanol and 50  $\mu$ L Nafion (5wt%) by ultrasonic treatment for 30 minutes to achieve a homogenous catalyst ink. Then 50  $\mu$ L catalyst ink was dropped uniformly onto the conductive fluorine-doped tin oxide (FTO) substrate, furnishing the working electrode. Detailly,

Cu-DBC/FTO, Pt wire, and Ag/AgCl were used as working electrode, counter electrode and reference electrode to form a three-electrode system. All the electrode potentials were measured against a Ag/AgCl electrode and converted to reversible hydrogen electrode (RHE) based on the following equation:

$$E_{RHE} = E_{Ag/AgCl} + 0.197 V + 0.059 \times pH$$

A 0.1 M KHCO<sub>3</sub> aqueous solution was used as the electrolyte and the pH value for 0.1 M CO<sub>2</sub>-saturated KHCO<sub>3</sub> solution is 6.8. Before the electrochemical measurements, high purity of CO<sub>2</sub> was purged into the H-type cell for 30 minutes at a flow rate of 20 ml/min. The reaction products were injected every 20 minutes and monitored by a gas chromatography (Agilent 7890B) equipped with flame ionization detector (FID), and thermal conductivity detector (TCD). Specifically, H<sub>2</sub> was detected by TCD, and CH<sub>4</sub>, C<sub>2</sub>H<sub>4</sub> and CO were detected by FID. The Faradaic efficiency of gas products were calculated by the equation:

$$FE = \frac{PV}{T} \times \frac{\nu NF}{I}$$

In which, FE represents the faradaic efficiency for CH<sub>4</sub>, CO, H<sub>2</sub> or C<sub>2</sub>H<sub>4</sub>; P, V and T means the reaction pressure (1 atm), gas flow rate (20 ml/min) and reaction temperature (298.15 K), respectively; F and  $\nu$  represent Faradaic constant (96485 C/mol) and volume ratio of different gas products in the outlet gas from the electrolyzer; N and I represent the electron transfer number, which is 8 for CH<sub>4</sub>, 2 is for H<sub>2</sub> or CO, and current, respectively.

**Photo-coupled electrochemical CO<sub>2</sub> reduction measurements.** The photo-coupled electrochemical measurements were similar with the measurements of electrochemical measurements. All the measurements were carried out in an H-type cell with a quartz window, using a Cu-DBC/FTO working electrode, a Pt wire counter electrode, and an Ag/AgCl reference electrode. The working electrode was irradiated through the quartz window, under a 300 W Xe lamp, with a light intensity of 300 mW cm<sup>-2</sup>, and irradiated area of 1 cm<sup>2</sup>. The recorded potentials were converted to vs RHE, which were identical to that of electrochemical measurements. The detection of gas products was carried out on an online gas chromatography analytical instrument (Agilent 7890B).

**Photocurrent response of Cu-DBC.** The microcrystalline powder of Cu-DBC was coated on FTO substrate with Nafion binder to prepare the working electrode. The photo-responsive signals were measured under chopped light at the potential of -1.0 V *vs.* Ag/AgCl in a CO<sub>2</sub>-saturated 0.1 M Na<sub>2</sub>SO<sub>4</sub> solution.

**Mott-Schottky measurements.** The Mott-Schottky measurements were conducted with a CHI660E chemical workstation at different frequencies (500 Hz, 1000 Hz and 1500 Hz) and in an electrolyzer with a quartz window, using a Cu-DBC/FTO working electrode, a Pt wire counter electrode, and an Ag/AgCl reference electrode. A 0.1 M Na<sub>2</sub>SO<sub>4</sub> solution was used as the electrolyte.

**Computational methods.** All calculations were performed on Materials studio 5.5 package. The potential energy surfaces for CO<sub>2</sub>RR catalyzed by Cu-DBC were calculated through the periodic density functional theory (PDFT) method by the Dmol<sup>3</sup> module. The widely used generalized gradient approximation (GGA) with the Perdew-Burke-Ernzerhof (PBE) functional and TS for DFT-D correction were involved.

## Supplementary References

- 1 Varshney, S. K.; Nagayama, H.; Takezoe, H.; Prasad, V. Octasubstituted dibenzochrysenes: discotic liquid crystals with a twisted core. *Liq. Cryst.* **36**, 1409-1415. (2009)
- 2 Gurudayal et al. Si photocathode with Ag-supported dendritic Cu catalyst for CO<sub>2</sub> reduction. *Energy Environ. Sci.* **12**, 1068-1077. (2019)
- 3 Yang, D. et al. Visible-light-switched electron transfer over single porphyrin-metal atom center for highly selective electroreduction of carbon dioxide. *Nat. Commun.* **10**, 3844. (2019)
- 4 Yang, Z. et al. New insight into photoelectric converting CO<sub>2</sub> to CH<sub>3</sub>OH on the one-dimensional ribbon CoPc enhanced Fe<sub>2</sub>O<sub>3</sub> NTs. *Appl. Catal. B: Environ.* **156-157**, 249-256. (2014)
- 5 Lan, Y. Q. et al. Ultrastable Dioxin-Linked Metallophthalocyanine Covalent Organic Frameworks as Photo-Coupled Electrocatalysts for CO<sub>2</sub> Reduction. *Angew. Chem. Int. Ed.* (2020)
- 6 Zhou, B. et al. A GaN:Sn nanoarchitecture integrated on a silicon platform for converting CO<sub>2</sub> to HCOOH by photoelectrocatalysis. *Energy Environ. Sci.* **12**, 2842-2848. (2019)
- 7 Han, E. et al. Worm-like FeS<sub>2</sub>/TiO<sub>2</sub> Nanotubes for Photoelectrocatalytic Reduction of CO<sub>2</sub> to Methanol under Visible Light. *Energy Fuels* **32**, 4357-4363. (2018)
- 8 Wang, Y.; Chen, J.; Wang, G.; Li, Y.; Wen, Z. Perfluorinated Covalent Triazine Framework Derived Hybrids for the Highly Selective Electroconversion of Carbon Dioxide into Methane. *Angew. Chem. Int. Ed.* **57**, 13120-13124. (2018)
- 9 Shi, G. et al. Copper nanoparticle interspersed MoS<sub>2</sub> nanoflowers with enhanced efficiency for CO<sub>2</sub> electrochemical reduction to fuel. *Dalton Trans.* **46**, 10569-10577. (2017)
- 10 Wang, X.; Varela, A. S.; Bergmann, A.; Kuhl, S.; Strasser, P. Catalyst Particle Density Controls Hydrocarbon Product Selectivity in CO<sub>2</sub> Electroreduction on CuOx. *ChemSusChem* **10**, 4642-4649. (2017)
- 11 Yi, J. D. et al. Highly selective CO<sub>2</sub> electroreduction to CH<sub>4</sub> by in situ generated Cu<sub>2</sub>O single-type sites on a conductive MOF: stabilizing key intermediates with hydrogen bonding. *Angew. Chem. Int. Ed.* **59**, 23641-23648. (2020)
- 12 Weng, Z. et al. Active sites of copper-complex catalytic materials for electrochemical carbon dioxide reduction. *Nat. Commun.* **9**, 415. (2018)
- 13 Li, J. et al. Electrohydrogenation of Carbon Dioxide using a Ternary Pd/Cu<sub>2</sub>O-Cu Catalyst. *ChemSusChem* **12**, 4471-4479. (2019)